ACS APPLIED NANO MATERIALS

www.acsanm.org Article

Nanometer-Thick Ion-Selective Polyelectrolyte Multilayer Coatings to Inhibit the Disintegration of Inorganic Upconverting Nanoparticles

Emilia Palo,* Hongbo Zhang, Mika Lastusaari, and Mikko Salomäki

Cite This: *ACS Appl. Nano Mater.* 2020, 3, 6892−6898 Read Online

ACCESS | Metrics & More | Article Recommendations | Supporting Information

ABSTRACT: Protective and ion selective polyelectrolyte multilayer coatings from poly(sodium 4-styrenesulfonate) and poly(diallyldimethylammonium chloride) were manufactured on the $NaYF_4$:Yb^{3+},Er^{3+} upconverting nanoparticle surface. The ion selective coatings would be effective in hindering the disintegration of inorganic nanoparticle in an aqueous environment used in various applications such as *in vitro* assays and biomedical imaging. The disintegration is prominent especially in detrimental phosphate-based buffers. The effect of the used counteranion on the multilayer formation and the luminescent properties of the coated materials is discussed. The multilayer coating was confirmed with Fourier transform infrared spectroscopy, thermal analysis, and transmission electron microscopy. The behavior of the coated nanoparticles in aqueous environment was monitored by using fluoride ion selective electrode. We observed that the ion selective coatings prepared using fluoride or chloride as a counteranion were the most effective in slowing the disintegration of the nanoparticles. The deceleration in the disintegration process was observed also in phosphate-based buffer which emphasizes the ion selective properties of the multilayer coating. The upconversion luminescence measurements of the coated nanoparticles showed that coatings manufactured with bromide counteranion were most efficient in shielding the upconversion luminescence in solid state.

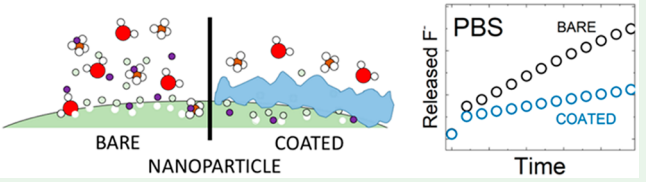

KEYWORDS: *nanoparticles, upconversion luminescence, layer-by-layer, polyelectrolytes, nanofiltering*

INTRODUCTION

The fluoride-based β-$NaYF_4$ structure is one of the most researched upconverting nanoparticle (UCNP) host materials to date. It is considered to be the most efficient nanoparticle in producing the visible luminescence when lanthanide ions (Yb^{3+}−Er^{3+} and Yb^{3+}−Tm^{3+}) are doped in the host lattice to replace Y^{3+} in the structure.[1,2] The visible light emission is obtained through stepwise energy transfer mechanism between the sensitizer (Yb^{3+}) and the activator (Er^{3+}/Tm^{3+}) ions when the upconversion material is excited with near-infrared radiation.[3,4] This property is widely researched for potential use in bioimaging, theranostics, and biomedical assays because the near-infrared radiation induces minimal light scattering and creates no interfering background from autofluorescence in biological matrices.[4−7] In addition, near-infrared radiation induces less damage to biological samples and penetrates deeper into tissue than the more commonly used ultraviolet radiation.

One of the most pressing challenges with the biocompatible fluoride-containing upconverting nanoparticles is their surface functionalization as the most commonly used syntheses yield nanoparticles have hydrophobic oleate surfaces.[5] While the surface functionalization eventually makes the nanoparticles dispersible in water for the use of applications such as biomedical assays and imaging, the actual contact with water reduces the emitted upconversion luminescence due to H_2O vibrational energy loss processes and buffer induced disintegration of the fluoride-containing inorganic nanoparticles in low concentrations.[8−12] Phosphate buffer is considered to be the most disruptive buffer for the fluoride containing nanoparticles as it can detach the lanthanide ions from the nanoparticle surface and form lanthanide phosphate and thereby increase the disintegration rate and change the surface topography of the nanoparticles.[13,14] Strategies to overcome the disintegration by adding additional fluoride into the storing solutions of the nanoparticles or creating coatings such as phosphonate coatings, amphiphilic polymers, polyelectrolyte multilayers, and polysulfonate cappings have been reported.[14−19]

Polyelectrolyte multilayers with varying structures have been studied in water-based applications as separation membranes due to their versatility in gas or liquid separation as well as nanofiltration.[20] Poly(sodium 4-styrenesulfonate) (PSS)/poly(diallyldimethylammonium chloride) (PDADMAC) multilayer

Received: May 7, 2020
Accepted: June 26, 2020
Published: June 26, 2020

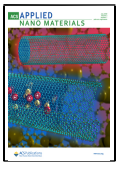

https://dx.doi.org/10.1021/acsanm.0c01245
ACS Appl. Nano Mater. 2020, 3, 6892−6898

structures have been reported to selectively separate fluoride, chloride, and phosphate ions.[21,22] This motivated us to study whether similar coatings could be manufactured on the $NaYF_4$:Yb^{3+},Er^{3+} UCNP surface by using the layer-by-layer technique as it would be beneficial to block the phosphate from the buffer to interact with the surface of the inorganic nanoparticle. To study the effect of the coating on the UCNP core material, a number of bilayers from PSS and PDADMAC polymers were manufactured on the UCNP surface. Because the counterion used in the polyelectrolyte solutions affects the swelling properties of the thin film, we used NaBr, NaCl, or NaF to adjust the ionic strength of the polyelectrolyte solutions and studied their effect on the coating.[23,24]

MATERIALS AND METHODS

Reagents. Poly(sodium 4-styrenesulfonate) (PSS; M_w 70000 $(C_8H_7NaO_3S)_n$, Aldrich), poly(diallyldimethylammonium chloride) (PDADMAC; 20 wt % in H_2O, M_w 100000−200000, $(C_6H_{16}ClN)_n$, Aldrich), sodium fluoride (NaF, 99%, Fluka), sodium bromide (NaBr, 99%, Alfa Aesar), sodium chloride (NaCl, 99.8%, VWR Chemicals), potassium chloride (KCl, 99.5%, Emsure), disodium hydrogen phosphate dodecahydrate ($Na_2HPO_4{\cdot}12H_2O$, 99%, Merck), and potassium dihydrogen phosphate (KH_2PO_4, cryst. extra pure, Merck) were used. The phosphate-buffered saline solution (PBS) with 10 mM HPO_4^- was prepared according to the protocol from Cold Spring Harbor Laboratory Press.[25]

Materials Preparation. The upconverting nanoparticles with a composition of $NaYF_4$:Yb^{3+},Er^{3+} (x_{Yb}: 0.17; x_{Er}: 0.03) were prepared with the high-temperature coprecipitation method.[26] The crystallite size of the hexagonal structured UCNPs was ca. 23 × 28 nm (width × length) calculated from the X-ray powder diffraction patterns with the Scherrer equation (Table S1 and Figure S1).[27] To prepare the UCNPs for the layer-by-layer coating, the hydrophobic oleic acid ligands on the UCNP surface were removed with an acidic treatment.[28,29] The polyelectrolyte coating solutions were 10 mM PSS or PDADMAC (the monomer concentration of polyelectrolyte) solubilized into 0.1 M of NaBr, NaCl, or NaF (aq). With NaBr and NaCl salts an additional 10 mM of NaF(aq) was added to each coating solution used including the water used for washing to ensure the survival of the core particle during the coating.[18] The 10 mM NaF concentration is low enough that it does not interfere with the effect from 0.1 M counteranion solution. For the polymer solutions in which the ionic strength was adjusted with NaF(aq) no additional fluoride was used as the fluoride concentration was already high enough to ensure that the particle stays unharmed during the coating procedure.

The coating using layer-by-layer assembly was performed by a procedure described in our previous paper and presented in Scheme 1.[18] After varying the PSS and PDADMAC components during the layer manufacturing, we added an additional PSS layer as the outermost layer, making the total number of formed bilayers to 1.5, 3.5, 4.5, and 5.5 creating multilayers of $(PSS/PDADMAC)_nPSS$ where n equals the amount of bilayers before the outer PSS layer (1, 3, 4, or 5).

Scheme 1. Simplified Scheme of the First Cycle of the Coating Process for PSS and PDADMAC Used for the Upconverting Nanoparticles

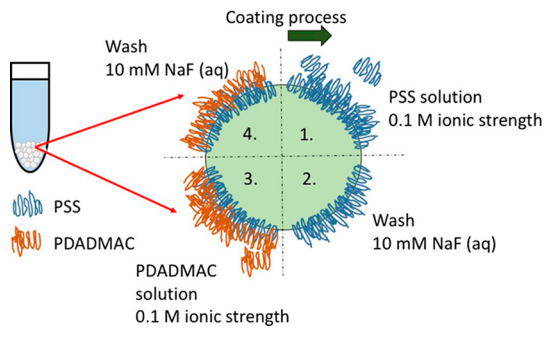

Characterization. The crystal structure of UCNPs was analyzed by X-ray powder diffraction (XRD) using a Huber G670 image plate Guinier camera (Cu $K\alpha_1$ radiation 1.5406 Å) at room temperature. The measurement range in 2θ was 4°−100° (step 0.005°), and the data collection time 30 min was followed by 10 data reading scans of the image plate. From the obtained data the crystallite size of the UCNPs was calculated with Scherrer formula by using reflections (002) for the thickness and (200) for the length of the hexagonal faces.[27] The Fourier transform infrared (FT-IR) spectroscopy was used to study the removal of the oleic acid and the growth of polyelectrolyte coating on the UCNP surface. A Bruker Vertex 70 MVP Star Diamond setup with 32 scans between 450 and 4500 cm^{-1} was used with a resolution of 4 cm^{-1}. For the thermal analysis a thermogravimetric analysis with differential scanning calorimetry (TGA-DSC) was measured by using one measurement sample with a TA Instruments SDT Q600 TGA-DSC apparatus. A temperature range of 35−600 °C was used with a heating rate of 10 °C/min in air (100 mL/min). For this setup the error of weight is ca. 1%. The images of the UCNPs were obtained with a JEM-1400 Plus 120 kV transmission electron microscope (TEM) using an OSIS Quemesa 11 Mpix bottom mounted digital camera (University of Turku) and a JEOL JEM-2200FS 200 kV equipped with an energy-dispersive X-ray spectroscopy detector (EDS) (OtaNano Microscopy Center, Aalto University, Espoo, Finland).

The disintegration of the nanoparticles in aqueous environment was studied by using a fluoride selective electrode to measure the fluoride ions disintegrated from the inorganic structure. The measurements were made in both PBS and NaCl spiked H_2O (same as the PBS, 0.14 M NaCl(aq)). One milliliter of H_2O or PBS was added into known amount of nanoparticles (ca. 2 mg), and the dispersion was transferred into dialysis tube (MWCO 6−8 kDa). The dialysis tube and its contents were then added into the aqueous measurement solution of H_2O or PBS (total volume 50 mL), and the release of the fluoride ions into the solution was monitored automatically for 24 h. The obtained fluoride release curves were extrapolated to equilibrium (1000 h) by using the basic first- and second-order exponential growth functions in OriginLab 2016 software.

The luminescence of the nanoparticles was measured by using a IFC-975-008 continuous wave fiber laser (Optical Fiber Systems Inc.) with an excitation wavelength of 975 nm (10270 cm^{-1}). Measurements were made from dry materials stacked densely inside a rotating capillary tube by using a 90° measurement conformation between the excitation and the emission. For the upconversion luminescence a 750 short pass filter was used after the sample to exclude the laser. The signal was guided into an Avantes Avaspec HS-TEC spectrometer and measured for 20 ms by using 20 averaging scans. For the luminescence in the NIR-II region (900−1750 nm) a 850 long pass filter was used after the sample, and the signals were collected with an Avantes Avaspec NIR512-1.7-EVO spectrometer for 100 ms by using 10 averaging scans.

RESULTS AND DISCUSSION

Coating of the Nanoparticles. Successful layer-by-layer coating of β-$NaYF_4$:Yb^{3+},Er^{3+} upconversion nanoparticles (size ca. 23 × 28 nm) by using PSS/PDADMAC multilayers was performed following Scheme 1 after the removal of the oleic acid capping. After the coating the FT-IR spectra of the nanoparticles have the characteristic vibrations of the used polyelectrolytes in the coating (Figure S2). The 1040 and 1182 cm^{-1} vibrations can be assigned to symmetric an antisymmetric vibrations of SO_3^- in PSS.[30] The SO_3^- group is also expected to give rise to the 1410 cm^{-1} vibration. The 1010 and 1128 cm^{-1} vibrations are due to the benzene ring in PSS, the first from in-plane bending and the latter from in-plane skeleton

https://dx.doi.org/10.1021/acsanm.0c01245
ACS Appl. Nano Mater. 2020, 3, 6892−6898

vibrations. In addition to the benzene ring in PSS there are remaining C−H vibrations at 1465 cm^{-1} from PDADMAC and PSS backbone, indicating the possible oleic acid impurities on the core particle surface. The bending of C−N in PDADMAC is reported to occur at 1635 cm^{-1}, but as the area is also common for various other vibrations such as C═C bending, it is not as clear indication of the polyelectrolytes as the SO_3^{2-} group.[31,32]

The thermal analysis of the coated nanoparticles was used to confirm the growth of the coating on the nanoparticle surface. The increase in the coating could be observed as a mass decrease in the nanoparticles during heating due to organic components (Figure S3). In addition, decomposition of the polymer material can be observed by the differential thermal analysis as an increase in the temperature difference between 400 and 500 °C (Figure 1 and Figure S3). The differences in

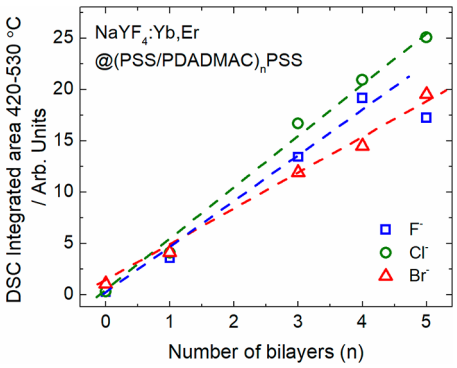

Figure 1. Integrated area of the 420−530 °C differential scanning calorimetry (DSC) temperature difference curve corresponding to the polyelectrolyte degradation with the number of coated bilayers with their respective counteranions (F^-, Cl^-, and Br^-). The lines are only a guide to the eye.

the peak shape with the counteranions F^- and Br^- when compared to Cl^- are expected to arise from the differences in the polymer composition within the bilayers as both layer components undergo disintegration close to 500 °C. It has been noted that in thin film formation on a flat surface the PDADMAC overcompensates and penetrates the PSS polymer structure deeper.[33] This results in a multilayer structure where there is more PDADMAC component present. It is possible that this kind of overcompensation is observable on these multilayers and that it begins earlier with multilayers prepared by using the Cl^- counteranion rather than F^- or Br^- in which the shoulder can be seen to disappear at 5.5 bilayers of coating. The overcompensation of PDADMAC could also be the reason for the larger mass decrease in the coatings made with the Cl^- counteranion.

To further clarify the presence of the multilayer coating, high-resolution TEM imaging was performed for the coated material with 5.5 bilayers of PSS/PDADMAC deposited with Cl^- counteranion as the thermal analysis suggested it to have the largest mass in the coating. The HR-TEM confirmed ca. 2 nm thick coating on the nanoparticle surface (Figure 2), explaining why it was not detectable from the normal TEM images (Figure S5). An EDS spectrum was also recorded to confirm the presence of the polymers on the material surface (Figure S6).

Survival of the Core Particles' Luminescence. Regardless of the number of coated bilayers or the counteranion used

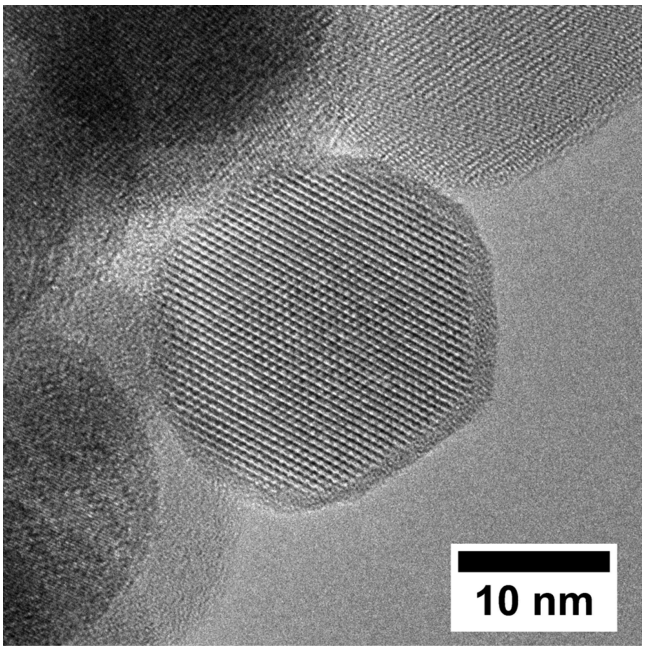

Figure 2. HR-TEM image of 5.5 bilayers of PSS/PDADMAC on the UCNP surface coated with Cl^- as the counteranion.

in the process, all coated nanoparticles showed the green ($^2H_{11/2}$, $^4S_{3/2}$ → $^4I_{15/2}$, Er^{3+}) and red ($^4F_{9/2}$ → $^4I_{15/2}$, Er^{3+}) upconversion luminescence obtained from the Yb^{3+}−Er^{3+} pair when excited at 975 nm (10256 cm^{-1}) (Figure S7). The small energy difference between the energy levels of $^2F_{5/2}$ (Yb^{3+}) and $^4I_{11/2}$ (Er^{3+}) with the laser excitation is the requisite of an efficient energy transfer mechanism behind the obtained upconversion luminescence. In addition, the conventional downshifting NIR II luminescence from $^4I_{13/2}$ → $^4I_{15/2}$ (Er^{3+}) can be observed from all of the materials (Figure S8).

As expected, the upconversion luminescence was enhanced up to certain number of bilayer coating due to the shielding of the core material and then again decreased due to quenching from interlocked water (Figure 3 and Figure S7).[12,19,34] The counteranion used in the coating process was expected to play a role also in the upconversion luminescence intensity due to the different hydration properties of the anions as well as their effect on the thickness and penetrability of the bilayers. With counteranions F^- and Cl^- the most efficient upconversion luminescence came with materials having $(PSS/PDADMAC)_4PSS$ structured coating on the surface. With Br^- the upconversion luminescence intensity was enhanced up to 5.5 bilayers of coating which differed from the other anions used. This would suggest that the Br^- binding to PDADMAC can keep the water molecules away from the core material and attached closer to the counterion in the coated polymer matrix.

The red-to-green (RtG) upconversion luminescence ratio can give information about the cross-relaxation processes that affect especially the green upconversion luminescence. With all of the counteranions the RtG ratio behaves similarly (Table S2) with the obtained upconversion luminescence, increasing up to a distinguished number of bilayers after the coating is grown on the surface. This suggests that there are interlocked water molecules within the structure which are participating the upconversion luminescence process by quenching the luminescence pathways.[12,34] When excitation power and upconversion luminescence intensity are plotted into a log−

https://dx.doi.org/10.1021/acsanm.0c01245
ACS Appl. Nano Mater. 2020, 3, 6892−6898

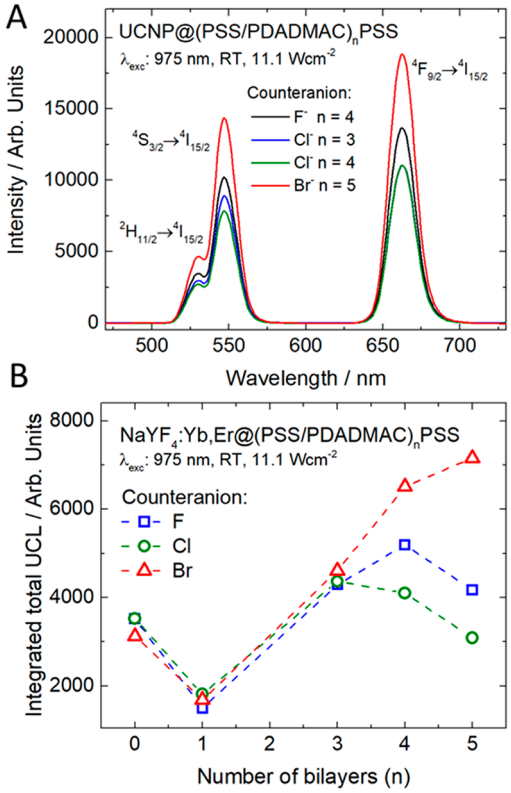

Figure 3. Upconversion luminescence spectra (λ_{exc}: 975 nm) of the most luminescent (PSS/PDADMAC)$_n$PSS-coated nanoparticles (A) and the integrated upconversion luminescence (UCL development with their respective number of bilayers (B) and the used counteranion.

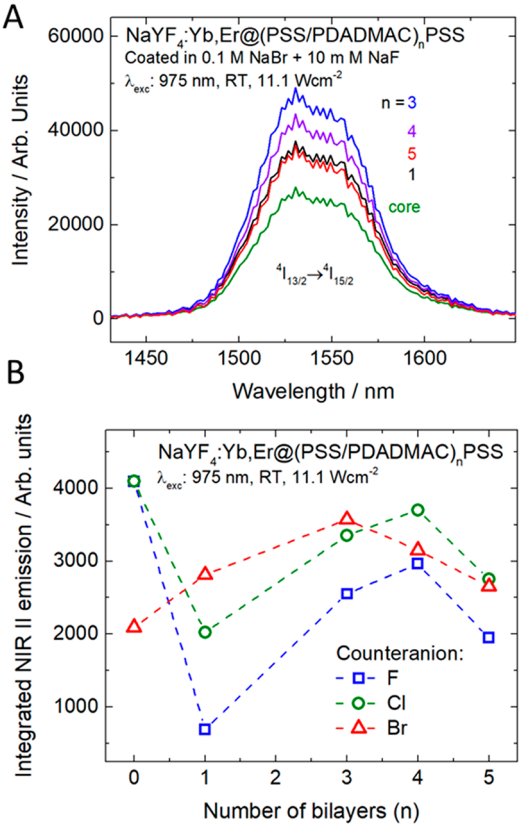

Figure 4. Downshifting luminescence spectra (λ_{exc}: 975 nm) of the (PSS/PDADMAC)$_n$PSS-coated nanoparticles with Br^- counteranion (A) and the integrated NIR II emission behavior (B) with their respective number of bilayers (n) and the used counteranion.

log scale and their slope is calculated, the value of the slope corresponds to the amount of needed photons to produce the measured upconversion luminescence. With the PSS/PDADMAC-coated materials the slopes for the green upconversion emission varied between 1.9 and 2.2 and for the red upconversion emission between 2.0 and 2.5 (Table S3). The slopes for the emissions were similar to those obtained previously so the coating was not expected to interfere with the upconversion luminescence process.[17,26]

The 1500 nm NIR emission ($^4I_{13/2} \rightarrow {}^4I_{15/2}$) from Er^{3+} obtained from the coated nanoparticles was weaker from that of the core material with all of the coatings made by using F^- and Cl^- as counteranions (Figure 4 and Figure S8). With the counteranion Br^- the coating improved also the 1500 nm emission up to 3.5 layers of coating. It is probable that the 1500 nm emission is more affected than the upconversion luminescence by the presence of even small amounts of water molecules. This is because the NIR emission (ca. 6540 cm^{-1}) can be quenched by just two water molecule phonons (ca. 3300 cm^{-1} each), whereas the level absorbing the 975 nm excitation (10255 cm^{-1}) in both the upconversion downshifting experiments would require more than three such phonons. This energy level is the $^2F_{5/2}$ of ytterbium that is responsible of the energy transfer and energy migration throughout the particle.[35]

Nanofiltration Properties of the Coating. Fluoride selective measurements were conducted to investigate whether the prepared PSS/PDADMAC multilayer coating was able to slow down the inorganic nanoparticle disintegration. As shown in Figure 5, the most efficient coating for slowing down the

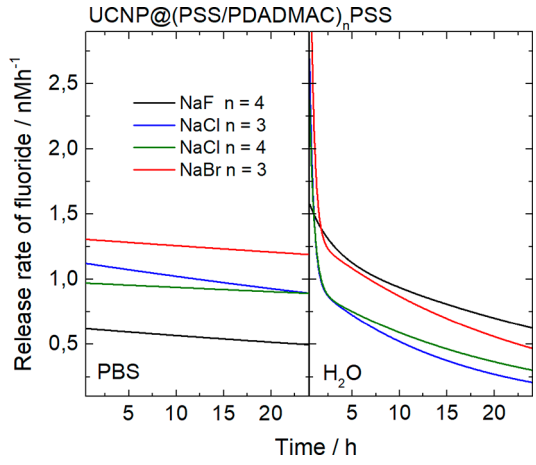

Figure 5. Fluoride release rate curves of the best PSS/PDADMAC coatings on the UCNP surface in PBS and NaCl spiked H_2O.

disintegration of inorganic core nanoparticles at the presence of the PBS was the material coated with (PSS/PDADMAC)$_4$PSS by using the fluoride counteranion. This is similar to the notion that adding fluoride ions into storage solutions of UCNPs prevents their disintegration.[10] As the PSS/PDADMAC multilayers have been reported to have both phosphate blocking properties and filtering monovalent ions, it is unclear which property plays the key role in slowing the disintegration in PBS while for the measurements in spiked H_2O only the monovalent ion filtration was expected to play a role.[21,22]

https://dx.doi.org/10.1021/acsanm.0c01245
ACS Appl. Nano Mater. 2020, 3, 6892−6898

The fluoride release curves obtained from the measurements made in NaCl spiked H_2O were similar to those obtained previously with different polyelectrolyte coatings on upconversion nanoparticles (Figure S10).[18] The shape of the fluoride release curves and the derivative of the release curves suggest that the fluoride release is controlled by the fluoride concentration in the solution as expected from the previous literature (Figures S10 and S11).[9,10,18] However, when the measurements were made in PBS, the shape of the curves (Figures S10 and S11) is almost linear, suggesting that the fluoride concentration has little or no effect on the disintegration of the nanoparticles in phosphate buffer. The disintegration of the inorganic nanoparticle structure in PBS is expected to be driven by the attack from the phosphate ions directly to the available surface lanthanide ions to form lanthanide phosphates.[9,15] This process subsequently exposes new fluoride ions available for disintegration. The filtration process and its deceleration can be seen as a change in the slope of the released fluoride as well as derivative release rates. The 10 mM additional fluoride used to prevent the particles from disintegrating during the coating process is also participating in the amount of released fluoride as well as the counteranion fluoride in comparison to the chloride and bromide used. Because of lack of resources only the most promising coatings were repeated for the measurement, but they performed similarly following the shape of the previously measured release curves. The error for this kind of ion selective *in situ* measurement is considered to be 10%, and this was minimized by calibrating the measurement setup before each measurement.

While the PSS/PDADMAC multilayer coating slows down the disintegration of the inorganic nanoparticle, the disintegration continues until an equilibrium in the fluoride concentration is reached. This equilibrium can, however, be reached also within smaller region such as the membrane structure of the coating instead of the total solution volume. It seems that the coatings made with presence of counteranions F^- and Cl^- are the most stable coating in water and phosphate buffer. For example, the 3.5 bilayers of (PSS/PDADMAC) coating made with Br^- counteranion seemed to slow down the disintegration process in the beginning when in contact with PBS. However, if the fluoride release was extrapolated to the equilibrium, it showed that the overall fluoride release from the same 3.5 bilayers of (PSS/PDADMAC) was almost 0.2 mM higher than that of the 4.5 bilayers of coating (Table S4). This suggests that there could be strong swelling within the multilayers when incubating in water since water molecules can replace the Br^- counteranion in the structure and interfere with the ion selective properties of the multilayers.[24,37]

CONCLUSIONS

We demonstrate that it is possible to grow ion selective polyelectrolyte multilayers with layer-by-layer coating as protective coating for upconversion nanoparticles. In addition, they hinder the disintegration process of the inorganic structure prominent in aqueous environments widely used in biomedical applications such as *in vitro* assays and bioimaging. Changing the counteranion during the coating process allowed to further affect the formation and selectivity of the multilayers. As expected, we found a threshold individual to the used counteranion in which the ion selectivity and deceleration of the disintegration was the strongest. The threshold number of bilayers 4.5 for fluoride was found to be similar to those reported with self-standing or on a flat substrate manufactured polymer multilayers.[21,22]

The strongest increase in upconversion luminescence intensity was obtained when the upconverting nanoparticles were coated with $(PSS/PDADMAC)_5PSS$ by using bromide as a counteranion. With fluoride or chloride as counteranion, the best upconverting luminescence intensity was obtained from $(PSS/PDADMAC)_4PSS$ and $(PSS/PDADMAC)_3PSS$, respectively. While the multilayers prepared by using bromide were promising in their luminescence, their behavior when exposed to aqueous environment showed that it is possible that the multilayer swelled and did not function as desired. When nanoparticles were exposed to PBS buffer, the material coated with $(PSS/PDADMAC)_4PSS$ by using fluoride as the counteranion was superior compared to others. However, its performance in NaCl spiked H_2O was not as good as the best chloride counteranion-coated multilayers.

Our study proves that nanofiltration through thin multilayer coatings could be used as a modification to decrease the disintegration of the upconverting nanoparticles in aqueous environments and especially in PBS. Further studies are needed to demonstrate the usability of these polymer-coated nanoparticles in different measurement matrices, but our study provides guidelines on the properties needed to be addressed when manufacturing this type of multilayer on nanoparticles.

ASSOCIATED CONTENT

Supporting Information

The Supporting Information is available free of charge at https://pubs.acs.org/doi/10.1021/acsanm.0c01245.

Additional characterization data for materials (XRD analysis, FT-IR spectra, thermal analysis, upconversion luminescence spectra) (PDF)

AUTHOR INFORMATION

Corresponding Author

Emilia Palo − *Department of Chemistry, University of Turku, FI-20014 Turku, Finland;* orcid.org/0000-0003-2367-8079; Email: emilia.palo@utu.fi

Authors

Hongbo Zhang − *Pharmaceutical Sciences Laboratory and Turku Bioscience Center, Åbo Akademi University, FI-20520 Turku, Finland;* orcid.org/0000-0002-1071-4416

Mika Lastusaari − *Department of Chemistry, University of Turku, FI-20014 Turku, Finland; Turku University Centre for Materials and Surfaces (MatSurf), FI-20014 Turku, Finland;* orcid.org/0000-0003-1872-0391

Mikko Salomäki − *Department of Chemistry, University of Turku, FI-20014 Turku, Finland; Turku University Centre for Materials and Surfaces (MatSurf), FI-20014 Turku, Finland;* orcid.org/0000-0001-6190-2073

Complete contact information is available at: https://pubs.acs.org/10.1021/acsanm.0c01245

Notes

The authors declare no competing financial interest.

ACKNOWLEDGMENTS

Financial support of E.P. from the Vilho, Yrjö and Kalle Väisälä Foundation and Turku University foundation is gratefully acknowledged. H.Z. acknowledges the Academy of Finland

(Grant 328933) for financial support. Markus Peurla (University of Turku) and Jiang Hua (Aalto University, Espoo, Finland) are thanked for the TEM images. This work made use of the Laboratory of Electron Microscopy premises at University of Turku as well as the provision of facilities and technical support by Aalto University at OtaNano - Nanomicroscopy Center (Aalto-NMC).

REFERENCES

(1) Suyver, J. F.; Grimm, J.; van Veen, M. K.; Biner, D.; Kramer, K. W.; Gudel, H. U. Upconversion Spectroscopy and Properties of $NaYF_4$ Doped with Er^{3+}, Tm^{3+} and/or Yb^{3+}. *J. Lumin.* **2006**, *117*, 1−12.

(2) Resch-Genger, U.; Gorris, H. H. Perspectives and Challenges of Photon-Upconversion Nanoparticles — Part I: Routes to Brighter Particles and Quantitative Spectroscopic Studies. *Anal. Bioanal. Chem.* **2017**, *409*, 5855−5874.

(3) Auzel, F. Upconversion and Anti-Stokes Processes with f and d Ions in Solids. *Chem. Rev.* **2004**, *104*, 139−173.

(4) Chen, G.; Qiu, H.; Prasad, P. N.; Chen, X. Upconversion Nanoparticles: Design, Nanochemistry, and Applications in Theranostics. *Chem. Rev.* **2014**, *114*, 5161−5214.

(5) Gorris, H. H.; Resch-Genger, U. Perspectives and Challenges of Photon-Upconversion Nanoparticles - Part II Bioanalytical Applications. *Anal. Bioanal. Chem.* **2017**, *409*, 5875−5890.

(6) Farka, Z.; Juřik, T.; Kovář, D.; Trnková, L.; Skládal, P. Nanoparticle-Based Immunochemical Biosensors and Assays: Recent Advances and Challenges. *Chem. Rev.* **2017**, *117*, 9973−10042.

(7) Dong, H.; Sun, L.; Yan, C. Energy Transfer in Lanthanide Upconverting Studies for Extended Optical Applications. *Chem. Soc. Rev.* **2015**, *44*, 1608−1634.

(8) Lisjak, D.; Plohl, O.; Ponikvar-Svet, M.; Majaron, B. Dissolution of Upconverting Fluoride Nanoparticles in Aqueous Suspensions. *RSC Adv.* **2015**, *5*, 27393−27397.

(9) Lisjak, D.; Plohl, O.; Vidmar, J.; Majaron, B.; Ponikvar-svet, M. Dissolution Mechanism of Upconverting AYF_4:Yb,Tm (A = Na or K) Nanoparticles in Aqueous Media. *Langmuir* **2016**, *32*, 8222−8229.

(10) Lahtinen, S.; Lyytikäinen, A.; Päkkilä, H.; Hömppi, E.; Perälä, N.; Lastusaari, M.; Soukka, T. Disintegration of Hexagonal $NaYF_4$:Yb^{3+}, Er^{3+} Upconverting Nanoparticles in Aqueous Media: The Role of Fluoride in Solubility Equilibrium. *J. Phys. Chem. C* **2017**, *121*, 656−665.

(11) Dukhno, O.; Przybilla, F.; Muhr, V.; Buchner, M.; Hirsch, T.; Mely, Y. Time-Dependent Luminescence Loss of Individual Upconversion Nanoparticles upon Dilution in Aqueous Solutions. *Nanoscale* **2018**, *10*, 15904−15910.

(12) Arppe, R.; Hyppänen, I.; Perälä, N.; Peltomaa, R.; Kaiser, M.; Würth, C.; Christ, S.; Resch-Genger, U.; Schäferling, M.; Soukka, T. Quenching of the Upconversion Luminescence of $NaYF_4$:Yb^{3+},Er^{3+} and $NaYF_4$:Yb^{3+},Tm^{3+} Nanophosphors by Water: The Role of the Sensitizer Yb^{3+} in Non-Radiative Relaxation. *Nanoscale* **2015**, *7*, 11746−11757.

(13) Plohl, O.; Kraft, M.; Kovac, J.; Belec, B.; Ponikvar-Svet, M.; Würth, C.; Lisjak, D.; Resch-Genger, U. Optically Detected Degradation of $NaYF_4$:Yb,Tm-Based Upconversion Nanoparticles in Phosphate Buffered Saline Solution. *Langmuir* **2017**, *33*, 553−560.

(14) Li, R.; Ji, Z.; Dong, J.; Chang, C. H.; Wang, X.; Sun, B.; Wang, M.; Liao, Y.-P.; Zink, J. I.; Nel, A. E.; Xia, T. Enhancing the Imaging and Biosafety of Upconversion Nanoparticles through Phosphonate Coating. *ACS Nano* **2015**, *9*, 3293−3306.

(15) Plohl, O.; Kralj, S.; Majaron, B.; Fröhlich, E.; Ponikvar-svet, M.; Makovec, D.; Lisjak, D. Amphiphilic Coatings for the Protection of Upconverting Nanoparticles against Dissolution in Aqueous Media. *Dalt. Trans.* **2017**, *46*, 6975−6984.

(16) Estebanez, N.; Gonzáles-Béjar, M.; Pérez-Prieto, J. Polysulfonate Cappings on Upconversion Nanoparticles Prevent Their Disintegration in Water and Provide Superior Stability in a Highly Acidic Medium. *ACS Omega* **2019**, *4*, 3012−3019.

(17) Palo, E.; Lahtinen, S.; Päkkilä, H.; Salomäki, M.; Soukka, T.; Lastusaari, M. Effective Shielding of $NaYF_4$:Yb^{3+}, Er^{3+} Upconverting Nanoparticles in Aqueous Environments Using Layer-by-Layer Assembly. *Langmuir* **2018**, *34*, 7759−7766.

(18) Palo, E.; Salomäki, M.; Lastusaari, M. Restraining Fluoride Loss from $NaYF_4$:Yb^{3+},Er^{3+} Upconverting Nanoparticles in Aqueous Environments Using Crosslinked Poly(Acrylic Acid)/Poly(Allylamine Hydrochloride) Multilayers. *J. Colloid Interface Sci.* **2019**, *538*, 320−326.

(19) Wilhelm, S.; Kaiser, M.; Würth, C.; Heiland, J.; Carrillo-Carrion, C.; Muhr, V.; Wolfbeis, O. S.; Parak, W. J.; Resch-Genger, U.; Hirsch, T. Water Dispersible Upconverting Nanoparticles: Effects of Surface Modification on Their Luminescence and Colloidal Stability. *Nanoscale* **2015**, *7*, 1403−1410.

(20) Nabeel, F.; Rasheed, T.; Bilal, M.; Iqbal, H. M. N. Supramolecular Membranes : A Robust Platform to Develop Separation Strategies towards Water-Based Applications. *Sep. Purif. Technol.* **2019**, *215*, 441−453.

(21) Hong, S. U.; Malaisamy, R.; Bruening, M. L. Separation of Fluoride from Other Monovalent Anions Using Multilayer Polyelectrolyte Nanofiltration Membranes. *Langmuir* **2007**, *23*, 1716−1722.

(22) Hong, S. U.; Ouyang, L.; Bruening, M. L. Recovery of Phosphate Using Multilayer Polyelectrolyte Nanofiltration Membranes. *J. Membr. Sci.* **2009**, *327*, 2−5.

(23) Salomäki, M.; Tervasmäki, P.; Areva, S.; Kankare, J. The Hofmeister Anion Effect and the Growth of Polyelectrolyte Multilayers. *Langmuir* **2004**, *20*, 3679−3683.

(24) O'Neal, J. T.; Dai, E. Y.; Zhang, Y.; Clark, K. B.; Wilcox, K. G.; George, I. M.; Ramasamy, N. E.; Enriquez, D.; Batys, P.; Sammalkorpi, M.; Lutkenhaus, J. L. QCM-D Investigation of Swelling Behavior of Layer-by-Layer Thin Films upon Exposure to Monovalent Ions. *Langmuir* **2018**, *34*, 999−1009.

(25) Phosphate-Buffered Saline (PBS), *Cold Spring Harb. Protoc.*, 2006.

(26) Palo, E.; Tuomisto, M.; Hyppänen, I.; Swart, H. C. H. C.; Hölsä, J.; Soukka, T.; Lastusaari, M. Highly Uniform Up-Converting Nanoparticles: Why You Should Control Your Synthesis Even More. *J. Lumin.* **2017**, *185*, 125−131.

(27) Klug, H. P.; Alexander, L. E. *X-Ray Powder Diffraction Procedures*; Wiley: New York, 1959.

(28) Palo, E.; Salomäki, M.; Lastusaari, M. Surface Modification of Upconverting Nanoparticles by Layer-by-Layer Assembled Polyelectrolytes and Metal Ions. *J. Colloid Interface Sci.* **2017**, *508*, 137−144.

(29) Bogdan, N.; Vetrone, F.; Ozin, G. A.; Capobianco, J. A. Synthesis of Ligand-Free Colloidally Stable Water Dispersible Brightly Luminescent Lanthanide-Doped Upconverting Nanoparticles. *Nano Lett.* **2011**, *11*, 835−840.

(30) De, R.; Lee, H.; Das, B. Exploring the Interactions in Binary Mixtures of Polyelectrolytes: Influence of Mixture Composition, Concentration, and Temperature on Counterion Condensation. *J. Mol. Liq.* **2018**, *251*, 94−99.

(31) Zhou, T.; Wang, M.; He, X.; Qiao, J. Poly(Vinyl Alcohol)/Poly(Diallyldimethylammonium Chloride) Anion-Exchange Membrane Modified with Multiwalled Carbon Nanotubes for Alkaline. *Fuel Cells. J. Mater.* **2019**, *5*, 286−295.

(32) Yang, D.-Q.; Rochette, J.-F.; Sacher, E. Spectroscopic Evidence for π-π Interaction between Poly(Diallyl Dimethylammonium) Chloride and Multiwalled Carbon Nanotubes. *J. Phys. Chem. B* **2005**, *109*, 4481−4484.

(33) Ghostine, R. A.; Markarian, M. Z.; Schlenoff, J. B. Asymmetric Growth in Polyelectrolyte Multilayers. *J. Am. Chem. Soc.* **2013**, *135*, 7636−7646.

(34) Hyppänen, I.; Perälä, N.; Arppe, R.; Schäferling, M.; Soukka, T. Environmental and Excitation Power Effects on the Ratiometric Upconversion Luminescence Based Temperature Sensing Using Nanocrystalline $NaYF_4$:Yb^{3+},Er^{3+}. *ChemPhysChem* **2017**, *18*, 692−701.

https://dx.doi.org/10.1021/acsanm.0c01245
ACS Appl. Nano Mater. 2020, 3, 6892−6898

(35) Hossan, Y.; Hor, A.; Luu, Q.; Smith, S. J.; May, P. S.; Berry, M. T. Explaining the Nanoscale Effect in the Upconversion Dynamics of β-$NaYF_4$:Yb^{3+}, Er^{3+} Core and Core−Shell Nanocrystals. *J. Phys. Chem. C* **2017**, *121*, 16592−16606.
(36) Salomäki, M.; Laiho, T.; Kankare, J. Counteranion-Controlled Properties of Polyelectrolyte Multilayers. *Macromolecules* **2004**, *37*, 9585−9590.
(37) Zerball, M.; Laschewsky, A.; Von Klitzing, R. Swelling of Polyelectrolyte Multilayers: The Relation Between, Surface and Bulk Characteristics. *J. Phys. Chem. B* **2015**, *119*, 11879−11886.

https://dx.doi.org/10.1021/acsanm.0c01245
ACS Appl. Nano Mater. 2020, 3, 6892−6898